Supplemental Material

The distribution of phosphorylated SR proteins and alternative splicing are regulated by RANBP2

Noriko Saitoh[*], Chiyomi Sakamoto[*], Masatoshi Hagiwara[†], Lourdes T. Agredano-Moreno[‡], Luis Felipe Jiménez-García[‡], Mitsuyoshi Nakao[*]

*Department of Medical Cell Biology, Institute of Molecular Embryology and Genetics, Kumamoto University, 2-2-1 Honjo, Kumamoto 860-0811, Japan
[†]Department of Anatomy and Developmental Biology, Kyoto University Graduate School of Medicine, Sakyo-ku, Kyoto, Japan
[‡]Department of Cell Biology, Faculty of Sciences, National Autonomous University of Mexico (UNAM), Mexico

Correspondence should be addressed to: norikos@kumamoto-u.ac.jp

Supplementary Methods

Antibodies

The primary antibodies used were: mouse SC35 (Sigma; 1:500), 1Sc4F11 (a gift from Dr. J. Stevenin, Institute de Genetique et de Biologie Moleculaire et Cellulaire, France), rabbit anti-DCP1A (a gift from Dr. J. Lykke-Andersen, University of Colorado, USA; 1:200), goat anti-TIA1 (Santa Cruz, c-20; 1:50), mouse anti-SR proteins mAb104 (ATCC, CRL-2067; 1:1), 1H4 (Zymed; 1:100), 3C5 (a gift from Dr. D. Spector, Cold Spring Harbor Laboratory, USA; 1:200), 16H3E8 (Zymed; 1:100), mouse anti-RNA polymerase II H5 (Covance; 1:10), CTD4H8 (Covance; 1:200), 8WG16 (Covance; 1:50), rabbit anti-RNA polymerase II phospho-S5 (Abcam; 1:500), mouse anti-phosphoserine PSR-45 (Sigma; 1:200), anti-phosphothreonine RTR-8 (Sigma; 1:200), goat anti-hnRNPA1 (Santa Cruz; 1:50), mouse anti-SF2/ASF 103 (Zymed; 1:200), human anti-hSm ANA-N (Sigma; 1:200), mouse anti-hnRNP C1/C2 4F4 (Santa Cruz; 1:1000), mouse anti-Y14 4C4 (Sigma; 1:400), human anti-fibrillarin (Sigma; 1:50), mouse anti-snRNA m3G (a gift from Dr. D. Spector, Cold Spring Harbor Laboratory, USA; 1:40), rabbit anti-Son WU14 (a gift from Dr. P. Bubulya, Wright State University, USA; 1:2000), mouse anti-SRPK1 (BD Transduction Laboratory; 1:1000), mouse anti-SRPK2 (BD Transduction Laboratory; 1:1000), rabbit anti-Clk1 (Abcam; 1:100), rabbit anti-Ranbp2–551 (a gift from Dr. T. Nishimoto, Kyushu University, Japan; 1:500), mouse anti-FLAG (Sigma, M5; 1:500), monoclonal rat anti-CD41 (Novus Biologicals, MWReg30; 1:500), and rabbit anti Histone H3 (Abcam; 1:1000). The following secondary antibodies were used: Alexa 488-conjugated donkey anti-mouse IgG (Molecular Probes; 1:250), Alexa 488-conjugated donkey anti-rabbit IgG (Molecular Probes; 1:250), Cy3-conjugated donkey anti-mouse IgG (Jackson ImmunoResearch; 1:1000), Cy3-conjugated donkey anti-rat IgG (Jackson ImmunoResearch; 1:1000), and Cy3-conjugated donkey anti-rabbit IgG (Jackson ImmunoResearch; 1:1000).

Primers for cDNA construction

pcDNA3-HA-NUP88-Region 1
Forward: 5′-TGCGCTAGCATGAGGCGCAGCAAGGCTGAC-3′
Reverse: 5′-GCAGCTAGCCTCGAGTTACAGATAATTTTTGCATTCTTCTTG-3′
pcDNA3-HA-NUP88-Region 2
Forward: 5′-TGCTCTAGAAGAAAGACCAGGGACTACCTA-3′
Reverse: 5′-GCATCTAGACTCGAGTTATTTCTTTGCAACCTGAAATTCAAA-3′
pcDNA3-HA-NUP88-Region 3
Forward: 5′-TGCTCTAGACATAAACCTATTGCAGAAGCTCCT-3′
Reverse: 5′-GCATCTAGACTCGAGTTATGATTTTTCACTACTAAAAATGCTTTT-3′
pcDNA3-HA-NUP88-Region 4
Forward: 5′-TGCTCTAGAATAGTTTCATTTGGATTTGGAAGT-3′
Reverse: 5′-GCATCTAGACTCGAGTTATATCTGTCCACATTCTGTGAT-3′
SR2/pcDNA3-FLAG-HA
Forward: 5′-CGGAATTCATGGAAGGAGCAAAGCCG-3′

Reverse: 5′-CCGCTCGAGAAGACATTCCTGGGTGAC-3′

siRNA sequences
RANBP2-7590: 5′-AACCAUUUGCAUUCGGCAA-3′
RANBP2-4777: 5′-GGCUCCAAAGAGCGGAUUU-3′
TNPO3-315: 5′-AUUGCUAAAGCCAGCUGCG-3′
TNPO3-1779: 5′-AGCUGUUGUCUCAAGAGCC-3′
RANGAP1-2544: 5′-AGCCUCUCCCAUCCCUUGG-3′
RANGAP1-3295: 5′-CCCAAAGCUGUUCUCCAGU-3′
SRPK1-236 (*SRPK1*-A): 5′-GAUACCAUGUGAUCCGAAA-3′
SRPK1-1867 (*SRPK1*-B): 5′-GCAGCUGGCUUCACAGAUU-3′
SRPK2-829 (*SRPK2*-A): 5′-GAGGCAGGCUGAGUUAUUG-3′
SRPK2-953 (*SRPK2*-B): 5′-UACUGCCCAGAGGUGAAAC-3′
RAN-68: 5′-ACGACCUUCGUGAAACGUC-3′
RAN-112: 5′-GUAUGUAGCCACCUUGGGU-3′
RAN-524: 5′-UUUGUUGCCAUGCCUGCUC-3′
SENP2-180: 5′-ACAGUCUCUACAAUGCUGC-3′
SENP2-234: 5′-AGCCCAUGGUAACUUCUGC-3′
PPP1CA: 5′-CCGCAUCUAUGGUUUCUAC-3′
PPP1CB: 5′-UUAUGAGACCUACUGAUGU-3′
PPP1CC: 5′-GCAUGAUUUGGAUCUUAUA-3′
PPP2CA-1: 5′-CGUGCAAGAGGUUCGAUGU-3′
PPP2CA-520: 5′-GAAUCCAACGUGCAAGAGG-3′
The siRNAs for *RCC1* and *SNUPN1* were purchased from Santa Cruz.
The siRNAs for *KPNA1* and *2*, *KPNB1*, *TNPO1*, *IPO5*, *XPO4*, *XPOT*, and *XPO1* were purchased from Applied Biosystems.
The siRNAs for *GL3* and *SUMO1*, *2*, and *3* were described previously (Saitoh *et al.*, 2006; Uchimura *et al.*, 2006).

Primers for RT-PCR
qPCR indicates quantitative PCR; the other primer sets were used for regular PCR.
CD44
Forward: 5′-CACCCGCTATGTCCAGAAAG-3′
Reverse to detect variants: 5′-CATTGAAAGAGGTCCTGTCC-3′
Reverse to detect standard: 5′-TGATTCAGATCCATGAGTGG-3′
CLK
Forward: 5′-GAGACCATGAAAGCCGGTAT-3′
Reverse: 5′-GCTTTATGATCGATGCACTC-3′
BCL2L1
Forward: 5′-GTAAAGCAAGCGCTGAGGGA-3′
Reverse: 5′-CATGGGCTGCATGTAGTGGT-3′
RANBP2
Forward: 5′-GGGATGTCAGTCAGTGGAAG-3′
Reverse: 5′-TATCTCCTCCTTGGCAAACA-3′

GAPDH
Forward: 5′-GATGCCCCCATGTTCGT-3′
Reverse: 5′-CAGGGGTCTTACTCCTTGGA-3′
RAN (qPCR)
Forward: 5′-AAGTTCAATGTATGGGACACAGC-3′
Reverse: 5′-CATCAAACATTATGATGGCACAC-3′
RANBP2 (qPCR)
Forward: 5′-TCCATTTTTCACAGAGTAATTCCA-3′
Reverse: 5′-CTGTTCCATCATGTTTGGTGA-3′
RCC1 (qPCR)
Forward: 5′-CCCAAAAGCAAGAAGGTGAA-3′
Reverse: 5′-TCGGGTTTTCTGGTCAGG-3′
RANGAP1 (qPCR)
Forward: 5′-AACTGTGGCATGGGCATT-3′
Reverse: 5′-CGGTGACATTCGGTCAGAG-3′
PP2CA (qPCR)
Forward: 5′-AGTTACACTGCTTGTAGCTCTTAAGGT-3′
Reverse: 5′-GCTCTCATGATTCCCTCGAA-3′
PP1CA (qPCR)
Forward: 5′-CCTATAAGATCAAGTACCCCGAGA-3′
Reverse: 5′-TGATGTTGTAGCGTCTCTTGC-3′
PP1CB (qPCR)
Forward: 5′-TGAACGTGGACAGCCTCAT-3′
Reverse: 5′-TCTTTCCTGGACGACATCCT-3′
PP1CC (qPCR)
Forward: 5′-CAACATCGACAGCATTATCCA-3′
Reverse: 5′-GACATTCTTACCAGGCTTGGAC-3′
TNPO3 (qPCR)
Forward: 5′-CCTACCAGATGTGGCTGAAGT-3′
Reverse: 5′-TCTAACCATCGACAAAAAGTCG-3′
SRPK1 (qPCR)
Forward: 5′-CCTCATTCAGGGGAAGAGTACA-3′
Reverse: 5′-CTGCCACAATGAGCTTGC-3′
SRPK2 (qPCR)
Forward: 5′-GGCACTTTGCTCTATCTGGAA-3′
Reverse: 5′-TCAGCTTGGTGATGTGTCG-3′
C-FOS (qPCR)
Forward: 5′-CTACCACTCACCCGCAGACT-3′
Reverse: 5′-AGGTCCGTGCAGAAGTCCT-3′
SENP2 (qPCR)
Forward: 5′-TGACAGTTACCCGAGATCAGC-3′
Reverse: 5′-GCCTTCTGAGTTCAAAGTAAAACC-3′
GAPDH (qPCR)

Forward: 5′-ACACCCACTCCTCCACCTTT-3′
Reverse: 5′-TAGCCAAATTCGTTGTCATACC-3′
ACTB (qPCR)
Forward: 5′-CCAACCGCGAGAAGATGA-3′
Reverse: 5′-CCAGAGGCGTACAGGGATAG-3′

Supplementary References

Caceres, J.F., Screaton, G.R., and Krainer, A.R. (1998). A specific subset of SR proteins shuttles continuously between the nucleus and the cytoplasm. Genes Dev *12*, 55-66.

Pinol-Roma, S., and Dreyfuss, G. (1992). Shuttling of pre-mRNA binding proteins between nucleus and cytoplasm. Nature *355*, 730-732.

Saitoh, N., Uchimura, Y., Tachibana, T., Sugahara, S., Saitoh, H., and Nakao, M. (2006). In situ SUMOylation analysis reveals a modulatory role of RanBP2 in the nuclear rim and PML bodies. Exp Cell Res *312*, 1418-1430.

Uchimura, Y., Ichimura, T., Uwada, J., Tachibana, T., Sugahara, S., Nakao, M., and Saitoh, H. (2006). Involvement of SUMO modification in MBD1- and MCAF1-mediated heterochromatin formation. J Biol Chem *281*, 23180-23190.

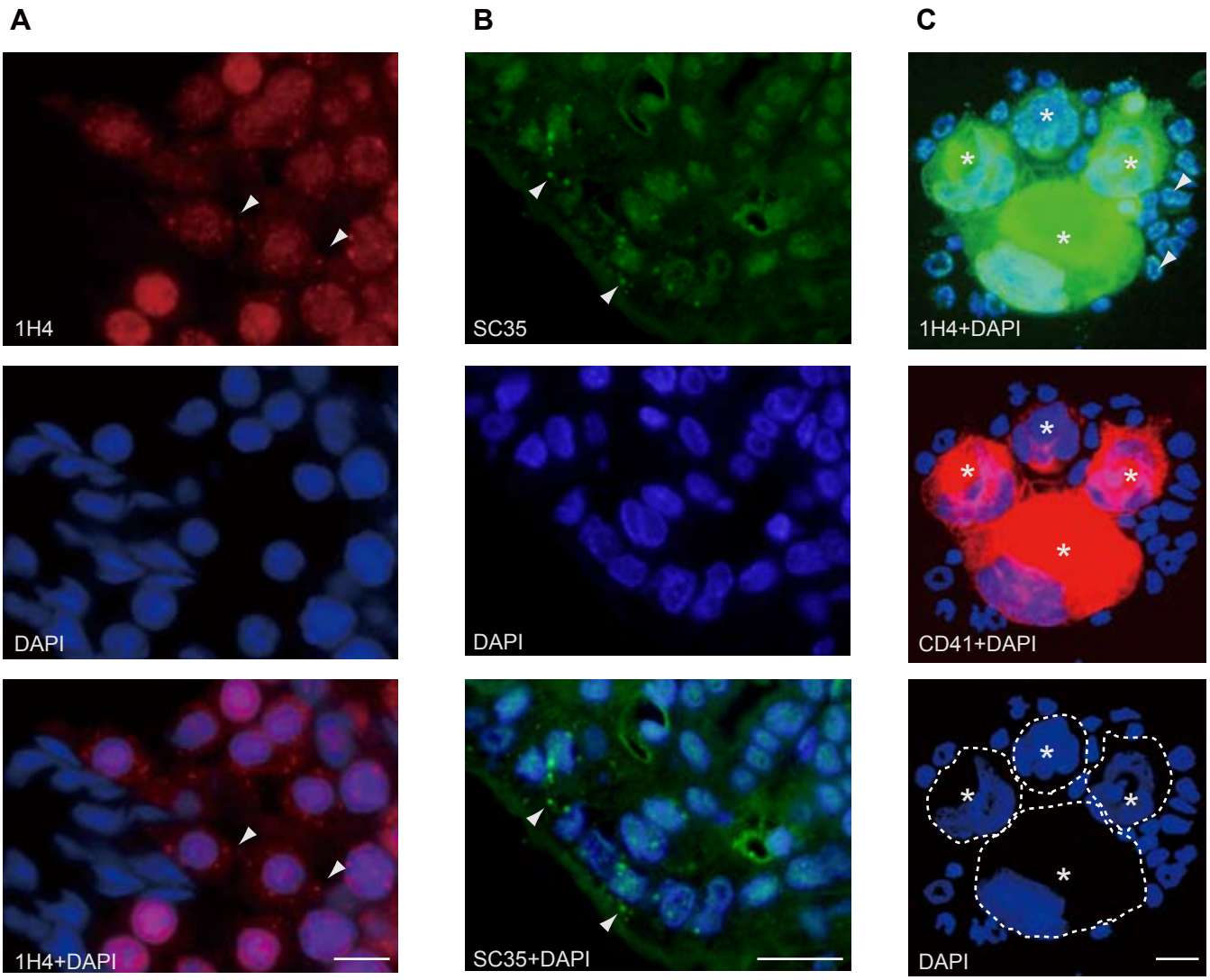

Figure S1. The subcellular distribution of phosphorylated SR proteins in various mouse tissues. (A) An adult mouse testis section was stained with monoclonal antibody 1H4 and DAPI. Phosphorylated SR proteins were distributed in a speckled pattern in the nucleus of spermatocytes, whereas they formed CGs in the spermatids (arrowheads), as was shown for SC35 in Figure 1. The bar represents 10 μm. (B) An adult mouse stomach section was stained with the monoclonal antibody SC35 and DAPI. A subpopulation of the surface epithelial cells in the gastric pits showed CG-like structures (arrowheads). The bar represents 20 μm. (C) A mixed population of cells derived from mouse bone marrow was stained with monoclonal antibody 1H4, CD41 (a megakaryocyte marker), and DAPI. The majority of phosphorylated SR proteins were located in the cytoplasm of megakaryocytes (asterisks), whereas they were located in the nuclear speckles of other blood cells (arrowheads). Megakaryocytes are delineated with dashed lines in the DAPI image. The bar represents 20 μm.

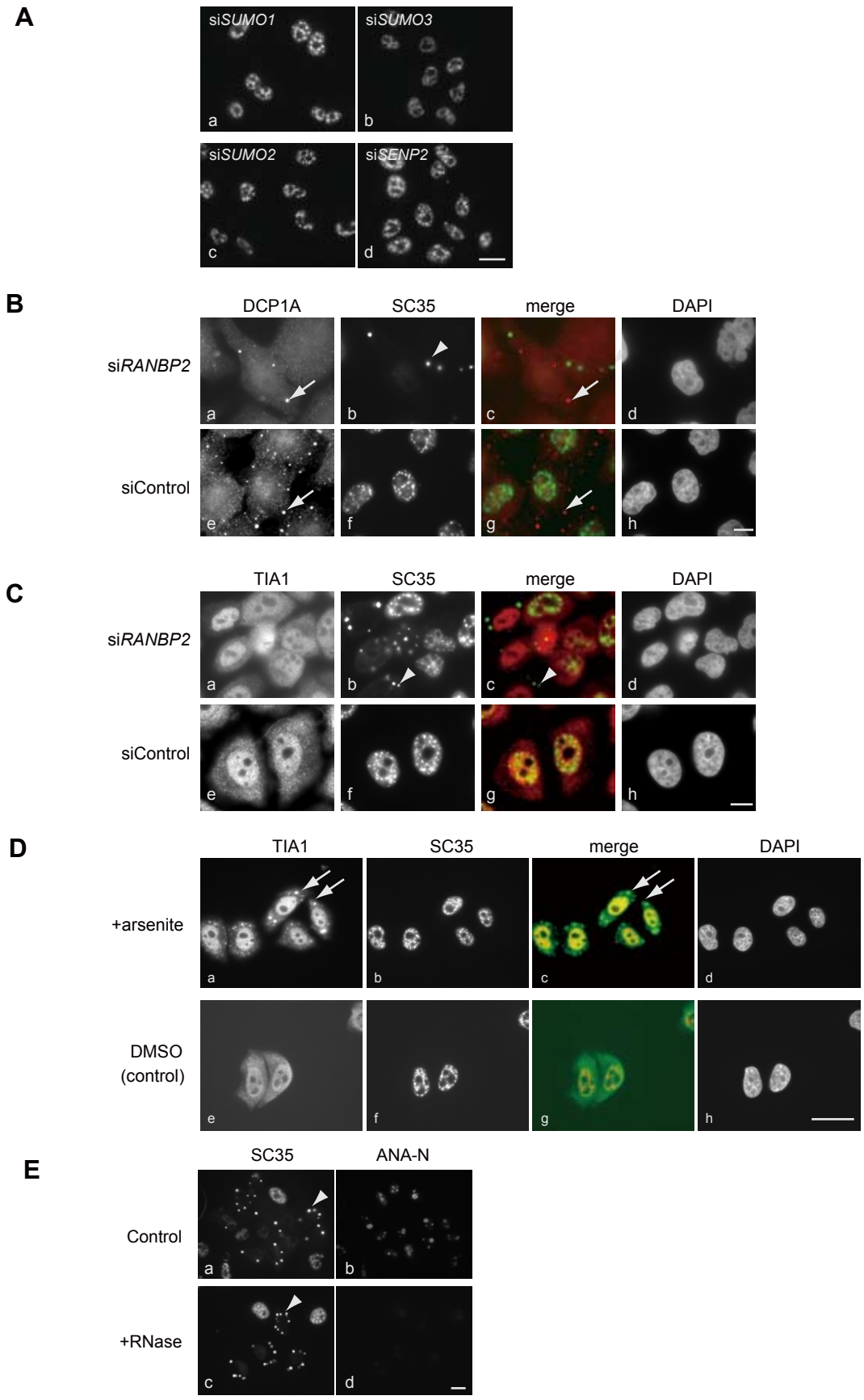

Figure S2. CGs do not colocalize with processing bodies or stress granules in mammalian cells. (A) HeLa cells were treated with siRNAs against factors involved in protein SUMOylation, followed by immunofluorescence with SC35 antibody. There were no remarkable changes in the nuclear speckles. (B–C) Decapping protein 1a (DCP1A), a component of processing bodies (arrows) (B) and T cell internal antigen 1 (TIA1), a component of stress granules (C) did not colocalize with CGs (arrowheads). (D) Stress granules (arrows) were induced in HeLa cells by treatment with 500 μM arsenite for 30 min, but the cellular localization of SC35 epitopes was not affected by the stress. (E) CGs (arrowheads) in RANBP2-knockdown cells were resistant to RNase treatment, in contrast to the nucleoli stained with ANA-N. The bars represent 10 μm (A–C and E) and 20 μm (D).

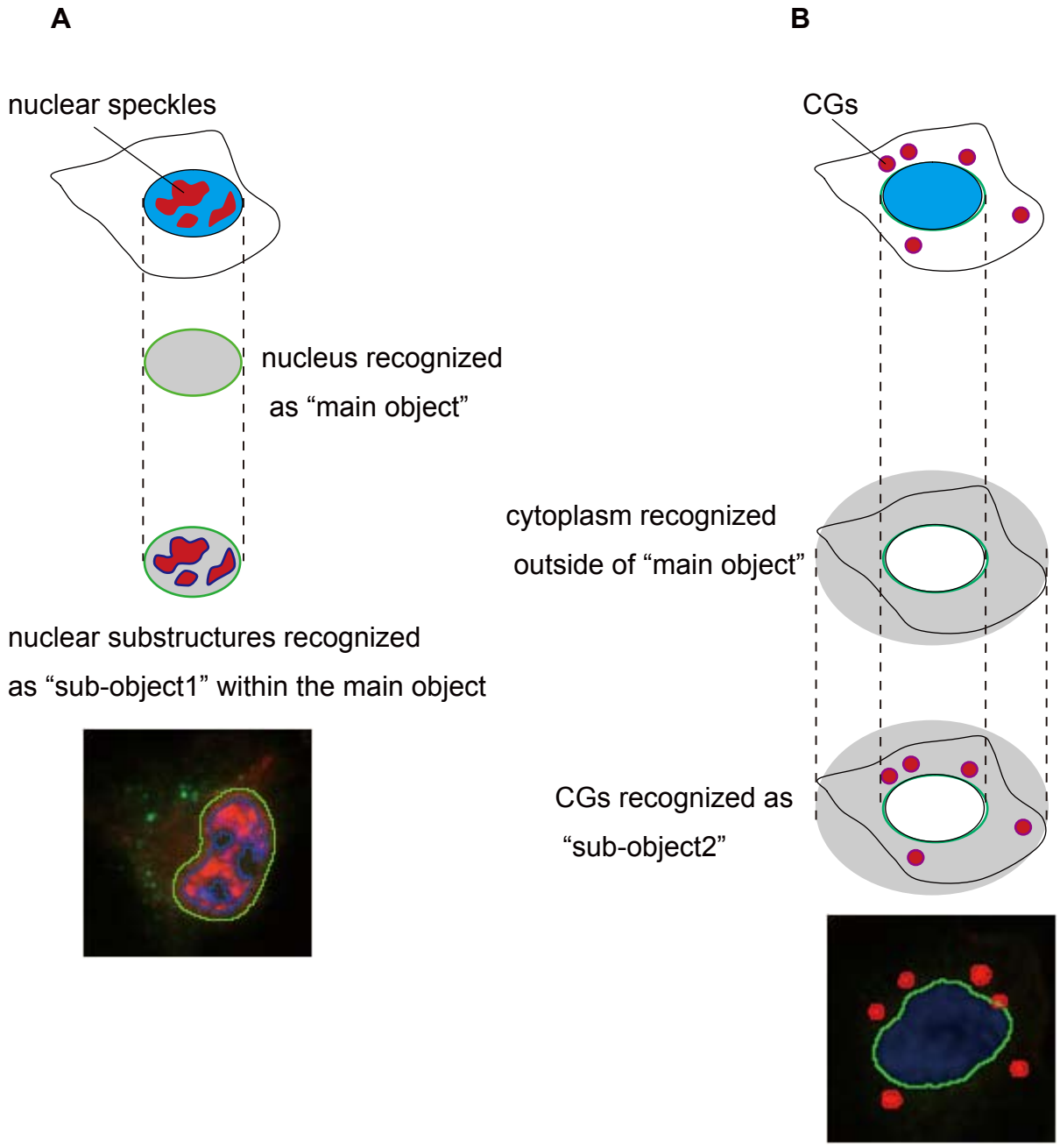

Figure S3. Automated analysis of nuclear speckle phenotypes. Nuclear speckles were automatically recognized by CELAVIEW analysis software that we developed in-house. (A) In merged DAPI- and SC35-stained digital images, the region containing DAPI staining, whose fluorescence intensity and area were within pre-determined ranges, was defined as the “main object” (outlined in green). SC35 signals inside the main object were then each defined as “sub-object 1” (outlined in blue). (B) CGs were recognized as SC35 signals within a fixed distance from the outer face of the nucleus, and were each defined as “sub-object 2” (outlined in red).

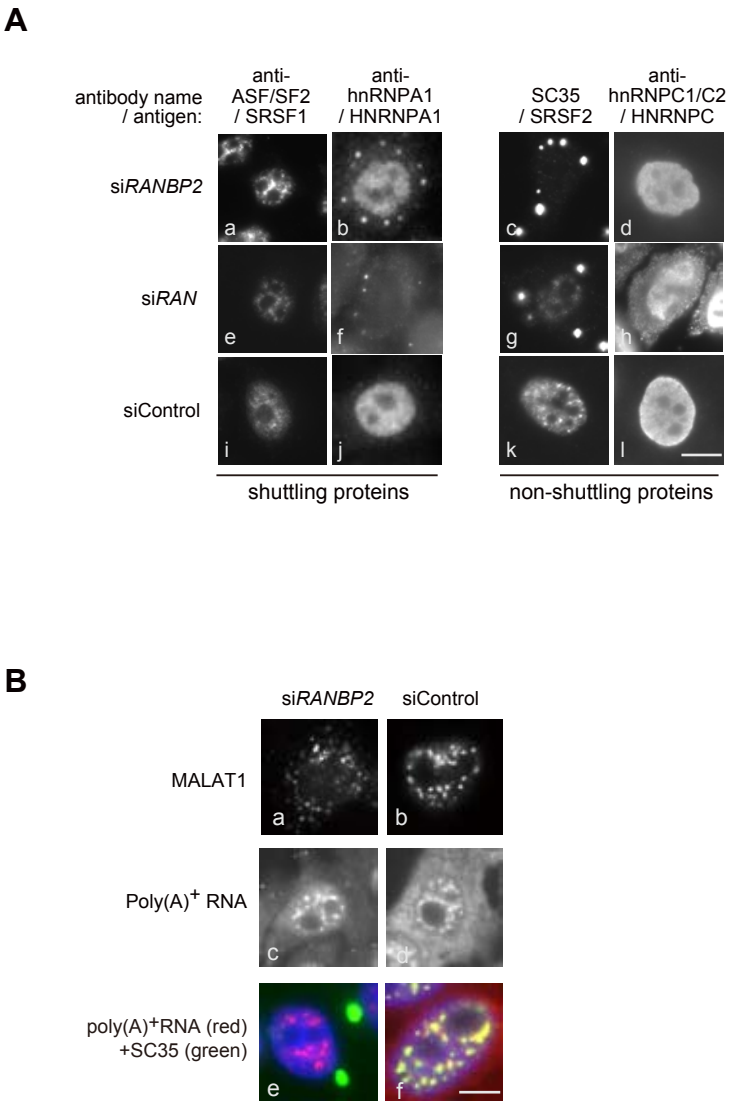

Figure S4. Characterization of cells with CGs. (A) CG localization does not directly depend on shuttling properties. Cells were stained with the indicated antibodies against shuttling and non-shuttling proteins (Pinol-Roma and Dreyfuss, 1992; Caceres *et al.*, 1998). (B) RNA-FISH of RANBP2-depleted HeLa cells showing poly(A)$^+$ RNAs and the long-nuclear-retained regulatory RNA, *MALAT1* (a–d). Immuno RNA-FISH was performed to simultaneously visualize poly(A)$^+$ RNAs (red) and SC35 antigens (green) (e, f). The bars represent 10 μm.

A

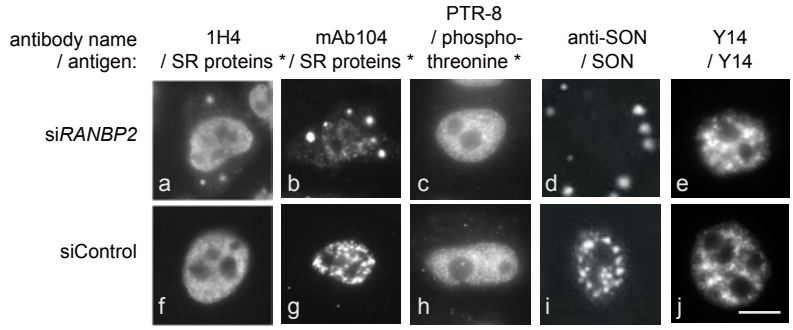

B

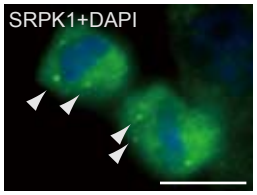

Figure S5. Immunofluorescence analyses of CGs and MIGs. (A) HeLa cells depleted of RANBP2 were immunostained as indicated. A series of phosphorylated SR proteins that are recognized by antibodies 1H4 (a, f) or mAb104 (b, g) were located in CGs, while phosphorylated threonines that are recognized by antibody PTR-8 were absent from CGs (c, h). (B) In normal HeLa cells, SRPK1 (green) localized in MIGs (arrowheads) at late telophase. DNA was counterstained with DAPI (blue). The bars represent 10 μm.

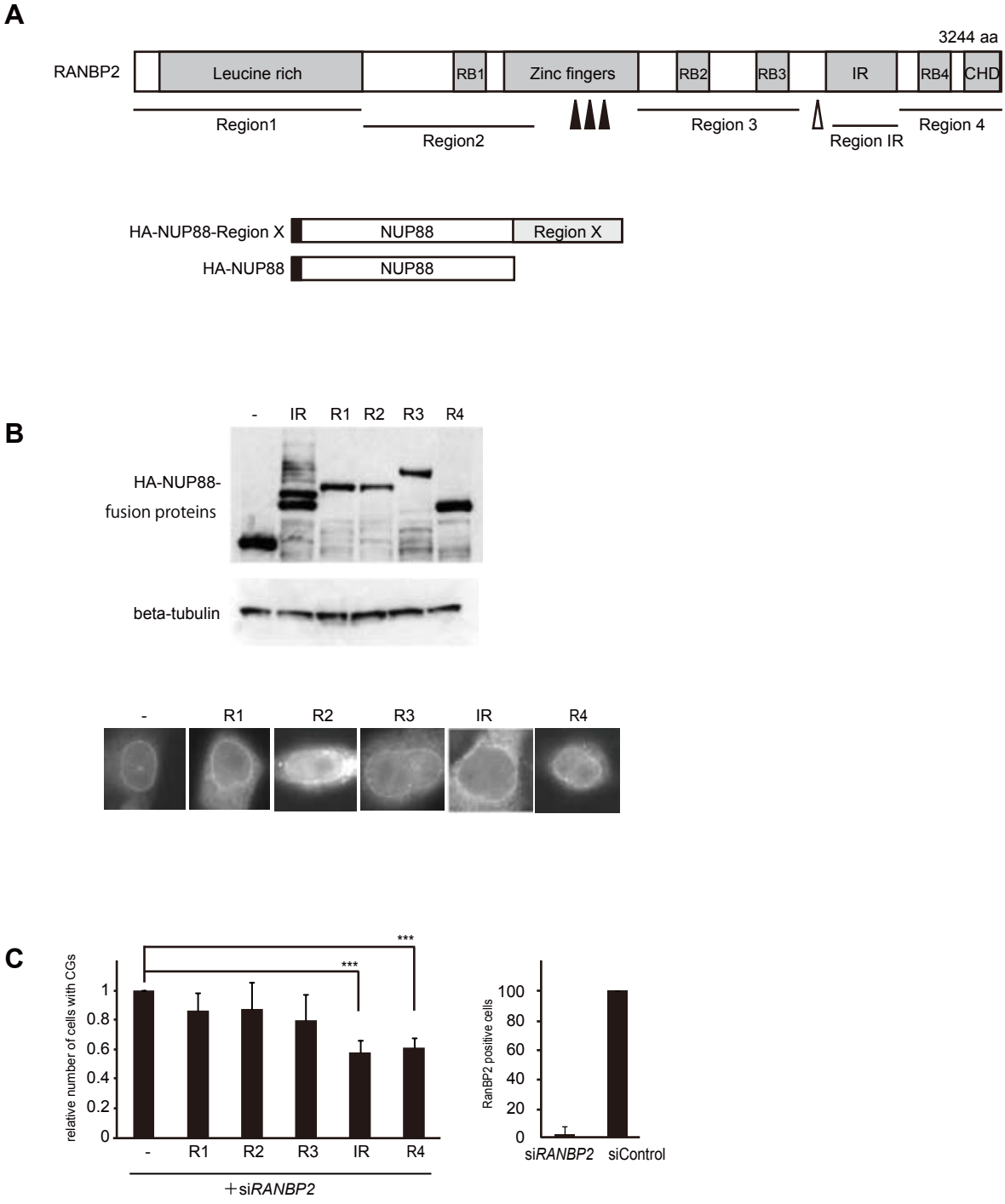

Figure S6. Partial recovery of nuclear speckles by re-introduction of sub-domains of RANBP2. (A) Primary structure of RANBP2 and its functional domains. RB1–4, Ran-binding (RANBP1-homologous) domain 1–4; IR, internal repeat domain (corresponding to the SUMO E3 domain); CHD, cyclophilin-homologous domain. Regions 1–4 or IR that were fused to NUP88 are indicated by the lines below. Filled triangles indicate the positions of the epitopes of the anti-RANBP2 antibodies; the unfilled triangle shows the position of the target sequence for the *RANBP2* siRNA. Plasmid constructs used for complementation tests are shown. Region X denotes Regions 1–4 or IR. The black box represents the hemagglutinin (HA) tag. (B) Confirmation of the exogenous expression and the nuclear pore complex localization of each fusion protein. Immunoblot probed with anti-HA tag (upper). Multiple bands shown above the HA-NUP88-IR fusion protein (second lane from the left) are poly-SUMOylated proteins, indicating that the fused IR domain was functional. Beta tubulin served as the loading control. Immunofluorescence with anti-HA antibody in cells transfected with the indicated fusion protein (lower). (C) The respective HA-NUP88-fusion proteins were expressed in RANBP2-knockdown cells, and immunofluorescence with SC35 was performed. The frequency of CG generation in cells expressing each fusion protein was counted and summarized (left). The values are the means and standard deviations of three independent experiments with more than 100 cells each. The introduction of the IR or Region 4 partially reduced CG generation (***$P < 0.001$), whereas the introduction of Regions 1, 2, or 3 had no significant effect ($P > 0.05$). Imaging cytometry analysis confirmed almost complete knockdown of endogenous RANBP2 (right).